Inhibited Release of Mobile Contaminants from Hanford Tank Residual Waste – 11447

Kirk J. Cantrell*, Steve M. Heald**, Bruce W. Arey*,
and Mike J. Lindberg*
* Pacific Northwest National Laboratory, Richland, Washington 99352
** Argonne National Laboratory, Argonne, Illinois 60439

ABSTRACT

Investigations of contaminant release from Hanford Site tank residual waste have indicated that in some cases certain contaminants of interest (Tc and Cr) exhibit inhibited release. The percentage of Tc that dissolved from residual waste from tanks 241-C-103, 241- C-106, 241-C-202, and 241-C-203 ranged from approximately 6 % to 10 %. The percent leachable Cr from residual waste from tanks C-103, C-202, and C-203 ranged from approximately 1.1 % to 44 %. Solid phase characterization results indicate that the recalcitrant forms of these contaminants are associated with iron oxides. X-ray absorption near edge structure analysis of Tc and Cr in residual waste indicates that these contaminants occur in Fe oxide particles as their lower, less soluble oxidation states [Tc(IV) and Cr(III)]. The form of these contaminants is likely as oxides or hydroxides incorporated within the structure of the Fe oxide.

Leaching behavior of U from tank residual waste was studied using deionized water, and $CaCO_3$ and $Ca(OH)_2$ saturated solutions as leachants. The release behavior of U from tank residual waste is complex. Initial U concentrations in water and $CaCO_3$ leachants are high due to residual amounts of the highly soluble U mineral čejkaite. As leaching and dilution occur $NaUO_2PO_4 \cdot xH_2O$, $Na_2U_2O_7$(am) and schoepite (or a similar phase) become the solubility controlling phases for U.

In the case of the $Ca(OH)_2$ leachant, U release from tank residual waste is dramatically reduced. Thermodynamic modeling indicates that the solubility of $CaUO_4$(c) controls release of U from residual waste in the $Ca(OH)_2$ leachants. It is assumed the solubility controlling phase is actually a hydrated version of $CaUO_4$ with a variable water content ranging from $CaUO_4$ to $CaUO_4 \cdot (H_2O)$. The critically reviewed value for $CaUO_4$(c) (log K_{SP}^0 = 15.94) produced good agreement with our experimental data for the $Ca(OH)_2$ leachates.

INTRODUCTION

At the U.S. Department of Energy's (DOE) Hanford Site in southeastern Washington State, large volumes of radioactive waste generated through reprocessing of spent fuel were stored in 177 single- and double-shell underground waste storage tanks. Most of these tanks (149) consisted of single-shell, steel and concrete storage tanks. The single-shell tanks (SSTs) are presently being retrieved to meet *Hanford Federal Facility Agreement and Consent Order – Tri-Party Agreement* Action Plan Milestone M-45-00, which states "…*retrieval of as much tank waste as technically possible, with tank waste residues not to exceed 360 cubic feet (Cu. Ft.) in each of the 100 Series tanks, 30 Cu. Ft. in each of the 200 Series tanks, or the limit of waste retrieval technology capability, whichever is less.*" This is equivalent to approximately 1 in. of residual waste remaining in the tank at closure. Pacific Northwest National Laboratory (PNNL) has completed chemical analysis, phase characterization, and leach testing of residual waste from four retrieved Hanford Site sludge SSTs; 241-C-103, 241-C-106, 241-C-202, and 241-C-203; one salt cake SST (241-S-112), and one partially retrieved sludge SST (241-C-108) to support closure of the SSTs as part of its Residual Tank Waste Contaminant Release Project funded by Washington River Protection *Solutions* LLC. For expediency, the tank designations will not include the 241 prefix from this point forward.

PNNL is taking a multi-tiered approach to study these residual wastes. Tier 1 tests focus on general characterization of the residual wastes (e.g., concentration measurements of contaminants and major components in the bulk residual waste), crystalline phase identification by X-ray diffraction (XRD), and identification of water-leachable constituents. Tier 2 analyses augment this characterization work and endeavor to determine the controlling mechanisms for release of contaminants. Tier 2 tests include selective extractions to quantify the release of contaminants from particular solid phases; scanning electron microscopy/energy dispersive spectrometry (SEM/EDS); and other techniques, such as synchrotron-based X-ray analysis, to identify phases in the as-received samples of residual wastes and solids remaining after the water leach and selective extraction studies.

A major project component is to develop release models for the residual waste that can be used in performance assessment models to evaluate the long-term risks to human health and the environment associated with closure of underground storage tanks at the Hanford Site. Release of contaminants from residual waste was quantified by leaching with aqueous solutions, selective extractions, and thermodynamic modeling.

During some of the early characterization and release model development work, it was determined that significant fractions of certain contaminants that are typically very mobile were not soluble in some tank residual waste samples. Because of the potential important implications of these findings with regard to tank closure performance assessments, further investigations are being conducted to determine more detailed characteristics of the forms of these contaminants. Identifying the exact form of the contaminants has been challenging. This is because the contaminants often occur at trace concentrations and the residual wastes are chemically-complex assemblages of crystalline and amorphous solids that contain contaminants as discrete phases and/or co-precipitated within oxide phases. Results from some of our early work using selective extractions suggested that significant fractions of Tc were typically co-precipitated at trace concentrations in Fe oxide phases that could not be identified unambiguously [1]. SEM/EDS indicated that Cr was also associated with Fe oxide/hydroxide phases [2,3]. More recent analyses of residual waste from C-103 have revealed the presence of Tc-containing Fe oxide/hydroxide particles, which is believed to be the first direct evidence of Tc in solid phases in actual samples of Hanford Site pre-retrieval tank waste or post-retrieval residual waste. The presence of mineralized coatings such as Fe oxides/hydroxides or reaction products precipitated from contact with cement pore fluids on contaminant-containing particles could decrease their rate of dissolution, thereby delaying the release of contaminants until the coatings dissolve sufficiently to expose the underlying matrix to infiltrating pore fluids.

Recent analysis using synchrotron-based X-ray analysis techniques has revealed that the valence of Tc and Cr in SST C-103 waste are in the reduced +4 and +3 states. These oxidation states typically form relatively insoluble oxide/hydroxides. This finding can partially explain why significant fractions of normally quite mobile contaminants in tank residual waste are resistant to dissolution. These and other findings are discussed in more detail in the following sections.

CHARACTERIZATION AND TEST METHODS

Analytical and test methods used to characterize tank waste samples and leachates have been described in detail previously [2]. A brief overview is provided here. The elemental and contaminant concentrations of the wastes were measured by complete dissolution of the bulk residual waste solids using fusion-dissolution procedures and acid digestions. Digests and leachates were analyzed using a combination of methods, including inductively coupled plasma-mass spectrometry, inductively coupled plasma-optical emission spectroscopy, and several radiochemical analytical techniques. Because the two solid digestion methods require the addition of acids to fully solubilize the waste solids, they are not appropriate

techniques for determining the anion concentrations of the bulk residual waste. Anion concentrations of the bulk residual waste solids were estimated separately by adding results from sequential deionized (DI) water extracts of the bulk residual wastes. The anion concentrations in these extracts were measured using ion chromatography. This approach may underestimate the total quantities of anions in the sample, particularly for anions that can form insoluble precipitates. The carbon contents (total carbon and total inorganic carbon) of the wastes were determined with a Shimadzu carbon analyzer.

Solid phase characterization techniques that were routinely used include XRD and SEM/EDS. XRD was used to identify crystalline phases. SEM in combination with EDS and X-ray fluorescence element mapping techniques were used to characterize phase associations, morphologies, particle sizes, surface textures, and compositions of solid particles in the unleached and leached residual waste samples. In some cases, additional studies were conducted based upon the specific characteristics of particular residual waste samples. These activities have included selective extractions and synchrotron-based X-ray techniques.

The synchrotron-based X-ray analyses were completed on beamline 20-ID at the Advanced Photon Source (Argonne National Laboratory [ANL], Argonne, Illinois), and included X-ray absorption spectroscopy (XAS), such as XANES and extended X-ray absorption fine structure spectroscopy; micro X-ray fluorescence (μSXRF); and micro X-ray diffraction. The XANES and extended X-ray absorption fine structure spectroscopy analyses were used to provide information about the oxidation state and chemical bonds for certain elements in solid and solution samples. Micro X-ray fluorescence is used for mapping the distribution of element concentrations in samples at the micrometer to submicrometer scale, and is particularly sensitive for elements with large atomic numbers, such as U and Tc.

A major component of this project is the development of contaminant release models for residual waste that can be used in performance assessments to evaluate the long-term risks to human health, safety and the environment associated with closure of underground storage tanks at the Hanford Site. Leachants used in these studies include DI water, a $Ca(OH)_2$ saturated solution, and a calcite ($CaCO_3$) saturated solution. The $Ca(OH)_2$ leachant is used to simulate conditions associated with the tanks being filled with cement, and is intended to represent the composition of a pore fluid that has contacted fresh cement prior to contacting the residual waste. The calcite-saturated leachant is used to simulate a future scenario in which rain infiltrates through the vadose zone into the interior of the SSTs and then reacts with aged concrete that has undergone carbonation and become coated with calcite. The aqueous leaching experiments were conducted using both single contact experiments and sequential contact experiments. The single contact experiments typically included 1 day and 1 month contact periods. The sequential contact experiments typically included six stages in which the leachate solution was replaced with fresh leachant after each contact period. The contact periods were typically 1 day for the first 5 stages and 30 days for the sixth stage. All the leach tests were conducted at a solution to solid ratio of approximately 100.

Thermodynamic equilibrium modeling was used to determine mineral saturation indices (SIs) to identify solid phases potentially in equilibrium with the leachate compositions and to create stability field diagrams. The SI is defined as $SI = \log (Q/K_{SP})$, where Q is the activity product and K_{SP} is the mineral solubility product at equilibrium at the temperature of interest. Minerals with SI values near zero (within $\pm \sim 0.5$) are generally considered to be near equilibrium, more positive values are considered oversaturated, and more negative values are considered undersaturated with respect to the solution composition. Geochemist's Workbench® version 8.09 [4] was used to calculate the mineral SIs for the leachates and create stability field diagrams. Previous SI calculations [3] have been revised to include thermodynamic constants for a number of additional U solid phases as well as solution phase complexes. The thermodynamic database thermo.com.V8.R6+.dat was used for the modeling calculations. The database was augmented to include solubility products for čejkaite [$Na_4(UO_2)(CO_3)_3$] and

[$NaUO_2PO_4 \cdot xH_2O$] [5]; becquerelite [$Ca(UO_2)_6O_4(OH)6 \bullet 8H_2O$] [6], Na diuranate hydrate [$Na_2U_2O_7 \bullet xH_2O$] [7]; urancalcarite [$Ca(UO_2)_3(CO_3)(OH)_6 \bullet 3H_2O$] (estimated value) [8]; andersonite [$Na_2Ca(UO_2)(CO_3)_3 \bullet 5H_2O$] and leibigite [$Ca_2UO_2(CO_3)_3 \bullet 10H_2O$] [9,10]; and autunite [$Ca(UO_2)_2(PO4)_2$] [11]; and stability constants for the dissolved species $CaUO_2(CO_3)_3^{2-}$(aq) and $Ca_2UO_2(CO_3)_3^{0}$(aq) [12].

RESULTS AND DISCUSSION

In their oxidized forms, Tc(VII), U(VI), and Cr(IV) are weakly or non-adsorptive and very [Tc(VII) and Cr(IV)] or moderately [U(VI)] soluble, and thus mobile in environmental systems, relative to their more reduced oxidation states Tc(IV), U(IV), and Cr(III). Because of their mobility in the environment, high toxicity, and except for Cr, their long half-lives, Tc, U, and Cr are important contaminants of interest at the Hanford Site and other DOE sites. Therefore, it is of critical importance to DOE and its tank closure efforts to determine oxidation state, and phase or phase associations to predict leaching behavior and assess risk associated with leaving residual wastes in the underground tanks after decommissioning.

As part of our studies to characterize and develop release models for Hanford Site tank residual waste, leaching studies were conducted using simulated sediment and cement pore water solutions. In some of these studies, it has been determined that for some tank residual waste samples, significant fractions of important contaminants of interest including Tc, and Cr are resistant to leaching. Understanding the nature of the recalcitrant forms of these contaminants and their release mechanisms has important implications to assessment of these future risks and could provide a mechanism for immobilizing normally highly mobile contaminants in a variety of environmental settings throughout the DOE complex.

Technetium

For Tc in residual wastes collected from Hanford Site SSTs C-103, C-106, C-202, C-203, and S-112, it was discovered the majority of Tc in the waste was resistant to dissolution by the three leaching solutions (DI water, calcite or $Ca(OH)_2$ saturated solution). The amount of Tc that was leachable in samples from tanks C-103, C-106, and C-202 ranged from approximately 6 % to 10 % of the total Tc in these samples [2,3,13,14,15]. The percent leachable Tc from tank C-203 residual waste was either not detected or less than the estimated quantification limit [3]. For tank S-112, only one leaching test was conducted using DI water. In this case, the percent leachable Tc was 17 % [16].

Efforts to characterize the nature of the Tc in the residual waste suggest Tc is associated with Fe oxides. Fig.1 shows SEM images collected in backscattered electron emission mode showing Fe oxide/hydroxide particles containing high concentrations of Tc-99 determined by EDS in residual waste samples from tank C-103. Concentrations of Tc in these particles ranged from ~0.6 to ~1.0 wt%. The authors believe this is the first direct evidence of Tc in solid phases in actual samples of Hanford pre- retrieval tank waste or residual waste. Previous evidence for the association of Tc with Fe oxides/hydroxides was indirect. Cantrell et al. [1,17] concluded from the results of their selective extraction experiments that the recalcitrant fraction of ^{99}Tc in the pre-final retrieval tank C-203 and C-204 waste samples was incorporated into an Fe oxide/hydroxide solid phase. However, other published studies of pertechnetate (TcO_4^-) and perrhenate (ReO_4^-, as an analogue of pertechnetate) sorption and coprecipitation suggest the recalcitrant pertechnetate in tank wastes could also be associated with Al hydroxyoxides [18,19]. In the actual tank residual waste samples analyzed to date, no Tc was ever detected in any of the numerous Al oxyhydroxide particles analyzed by EDS. Recently published quantum-mechanical modeling of Tc-99 incorporation into hematite indicates that incorporation of small amounts of Tc(IV) (up to at least 2.6 wt. %) is energetically feasible whereas incorporation of pertechnetate (TcO_4^-) was unfavorable [20].

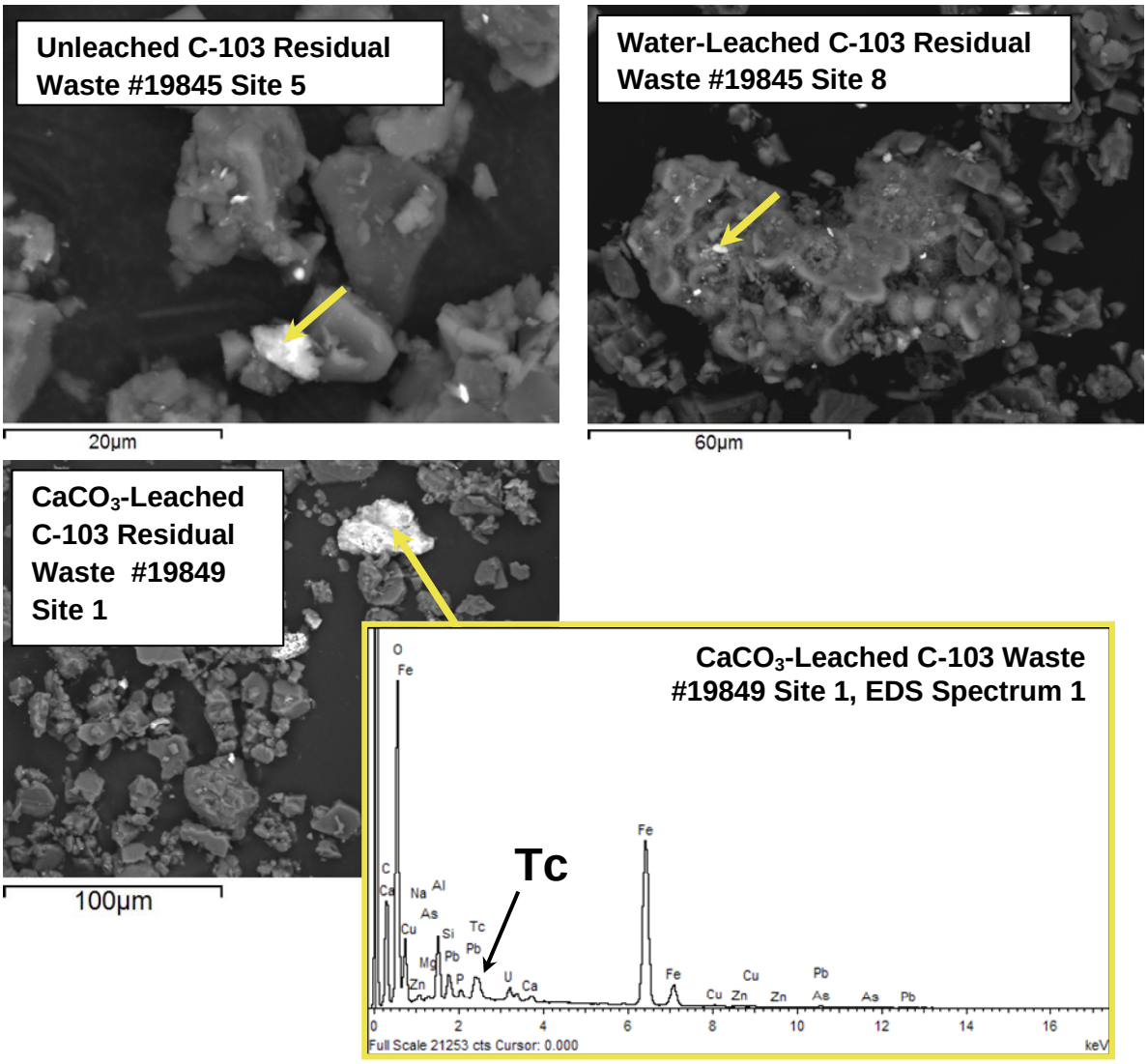

Fig. 1. SEM micrographs collected in backscattered electron emission mode showing Fe oxide particles containing high concentrations of ^{99}Tc determined by EDS in residual waste samples from SST C-103 [2].

To determine the oxidation state(s) of Tc in the tank C-103 residual waste, samples were analyzed using XANES at the Advanced Photon Source at ANL. Results of this analysis are shown in Fig. 2. Shown in Fig. 2 are the XANES spectra of one scan (scan 2), the average of three scans (scans 2-4), and three standards for comparison. The standards include Tc(VII) in the form of pertechnetate (TcO_4^-), Tc(IV) in the form of TcO_2, and Tc(IV) incorporated into the Fe hydroxide ferrihydrite. The spectra clearly indicate the Tc is in the +4 oxidation state. Because of the low concentration of Tc at the spot analyzed, the quality of the spectra were not high enough to differentiate between Tc(IV) in the form of TcO_2 or Tc(IV) incorporated into ferrihydrite. This result is, however, the first evidence that clearly demonstrates that Tc in tank residual waste is in the relatively insoluble +4 oxidation state and explains why much of the Tc that occurs in tank residual waste at the Hanford Site is recalcitrant to dissolution. This result was not expected a priori because the tank environment is exposed to the atmosphere and is generally oxidizing.

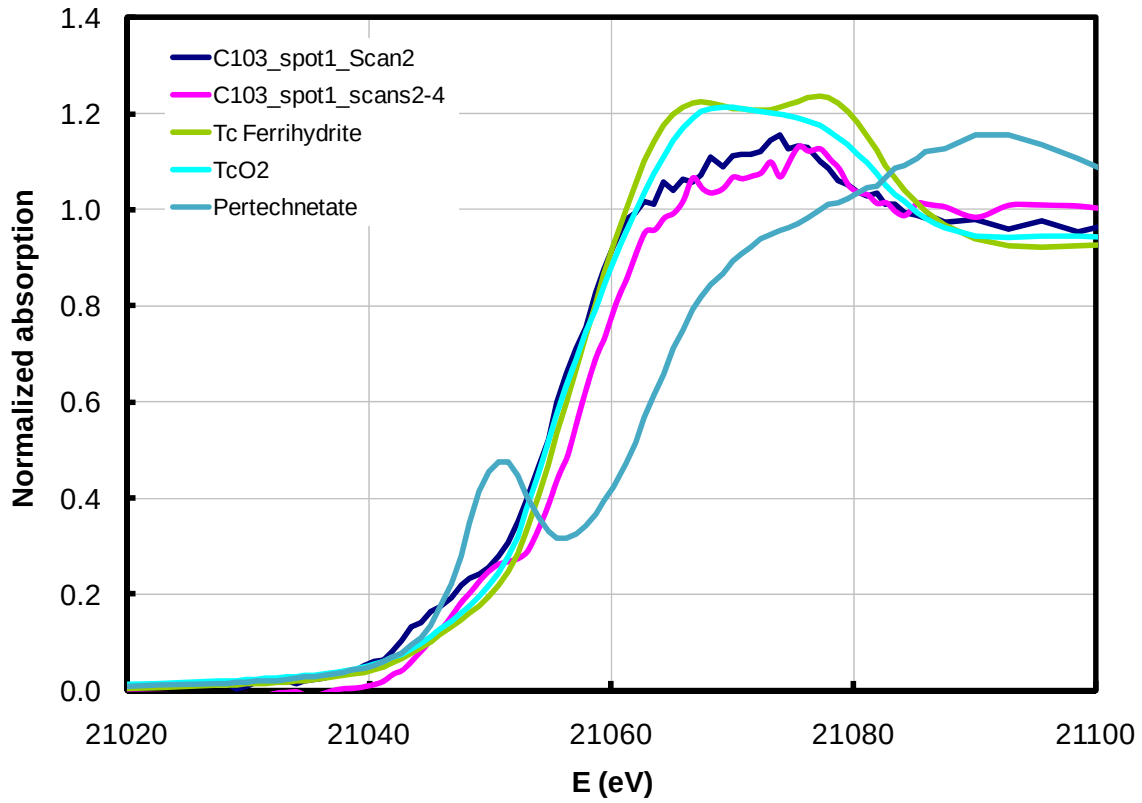

Fig. 2. XANES spectra collected for a high Tc concentration spot found in a SST C-103 residual waste sample.

Chromium

Similarly to Tc, major fractions of Cr in Hanford Site tank residual waste are resistant to dissolution. Table 1 shows results of the percent cumulative leachable Cr from sequential leach tests of residual waste from Hanford Site SSTs C-103, C-202, and C-203 [2,3,15]. Data for tank C-106 are not shown because Cr concentrations determined in both the residual waste and leachates were below the quantification limits [14]. Values in Table 1 that are in parenthesis are based on estimated values that were below the quantification limit in the leachates and are associated with greater uncertainty. The percent leachable Cr in these samples range from 1.1 % to 44 %.

Table 1. Percent cumulative leachable Cr from sequential leach tests of Hanford tank residual waste.

Tank ID	DI Water Leachant	$CaCO_3$ Leachant	$Ca(OH)_2$ Leachant
C-103	1.1 – 6.4	Below Detection	(3.7 – 4.7)
C-202	(5.9)	4.7	8
C-203	34 – 44	18 – 22	6 – 11
Parenthesis indicate measured values were below the estimated quantification limit			

Analysis of residual tank wastes from C-103, C-202, C-203 by SEM-EDS indicated that when Cr is detected, it is always associated with Fe oxides [2,3]. Previous studies were conducted to establish the oxidation state(s) of Cr in the tank C-106 residual waste. These samples were analyzed using XANES at the Advanced Photon Source at ANL. Results of these analyses indicated the majority of Cr in tank C-

106 residual waste was in the Cr(III) oxidation state [21]. To produce more conclusive evidence that Cr in Hanford Site residual waste occurs primarily as Cr(III), a C-103 residual waste sample was recently analyzed using XANES. The XANES spectra from three high Cr concentration spots in the sample are shown in Fig. 3, along with Cr(III) [Cr_2O_3] and Cr(VI) [CrO_4^{2-}] standards. Through comparison of these XANES spectra, it is readily apparent the three sample spots are consistent with Cr in the Cr(III) oxidation state. Based upon this evidence, the authors concluded the recalcitrant nature of Cr in Hanford Site tank residual waste is the result of its occurrence in the relatively insoluble Cr(III) oxidation state. In this oxidation state, Cr could exist as $Cr(OH)_3$, Cr_2O_3, or as a solid solution with various Fe oxide/hydroxides. All of these forms are relatively insoluble.

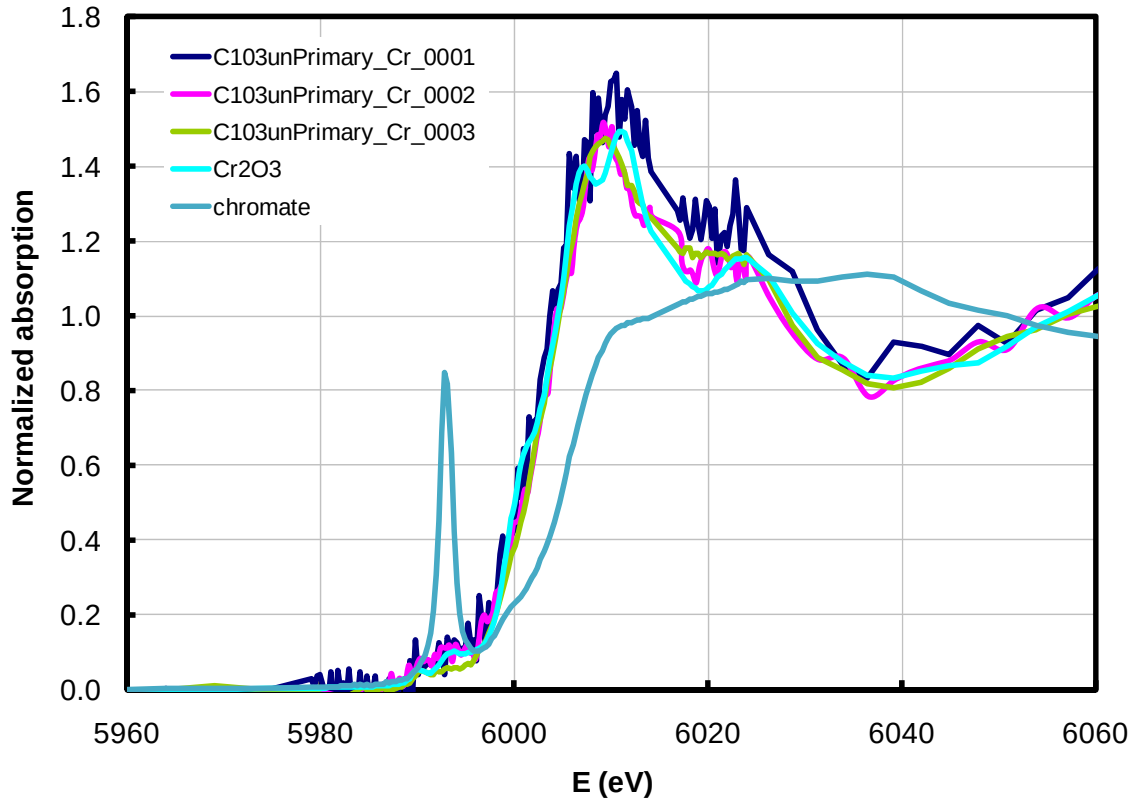

Fig. 3. XANES spectra collected at three high Cr concentration spots found in a sample of SST C-103 residual waste.

Uranium

The release behavior of U from Hanford Site residual waste is quite different from that of Tc and Cr. Uranium release varies considerably from tank to tank and is typically greatly affected by the type of leachant solution. Table 2 shows the release model data that have been developed to date for residual waste from SSTs C-103, C-106, C-202, and C-203. A particularly noteworthy feature of the U release data presented in Table 2 is the large differences in U leachability that occurs between the $CaCO_3$ leachants and the $Ca(OH)_2$ leachants. It is presumed the cause of this behavior is transformation of an initially Na rich U phase to a more Ca rich U phase, which has a much lower solubility. The identity of this phase(s) could not be positively identified.

Table 2. Current U release model data for residual waste from Hanford Site SSTs C-103, C-106, C-202, and C-203.

Tank	Maximum Waste Concentration (µg/g-waste)	Leachant Solution	Maximum Release Concentration (µg/L)
C-103	4,200	$Ca(OH)_2$	2.0
		$CaCO_3$	4,100
C-106	310	$Ca(OH)_2$	36
		$CaCO_3$	49
C-202	240,000	$Ca(OH)_2$	1,700
		$CaCO_3$	61,000
C-203	590,000	$Ca(OH)_2$	5,300
		$CaCO_3$	510,000

The values shown in Table 2 were determined empirically from leach test experiments and are conservative in that the maximum release concentrations were determined from the highest concentration of U measured in any of the leachate solutions. To illustrate this point, the U concentrations measured in the $CaCO_3$ sequential leach tests determined with tank C-203 residual waste are shown in Fig. 4. Aside from one outlier for contact number six, these data show the general trend is a substantial decrease in U concentrations during successive contacts, particularly for the early contact stages. The cause of this behavior is likely due to the presence of a minor amount of the highly soluble U phase čejkaite [$Na_4UO_2(CO_3)_3$] in the residual waste. Čejkaite was a major phase identified in the tank C-203 and C-204 pre-retrieval waste [1,22]. SEM images of tank C-203 pre-retrieval waste and post-retrieval residual waste collected in backscatter electron emission mode are shown in Fig. 5. On the right side of Fig. 5, hexagonal čejkaite crystals found in tank C-203 pre-final retrieval waste are shown. On the left side of Fig. 5, a U rich particle (Na-U-P from SEM-EDS) found in the C-203 post-retrieval residual waste is shown that contains hexagonal or rod-like dissolution cavities. This evidence supports our hypothesis that residual čejkaite in C-203 residual waste is responsible for the high U concentrations that occur in the initial stages of the leaching experiments.

Positive phase identification of U phases that occur in the as-received residual waste and the leached residual waste has been problematic. XRD analysis has indicated the major U phases that occur in the residual wastes are amorphous or are below the detection limit and thus cannot be identified by XRD. Although čejkaite was identified in SSTs C-203 and C-204 pre-retrieval wastes, its presence in post-retrieval wastes was below the detection limit of XRD and could not be verified. To more accurately predict future U releases from the final closed tanks, it is necessary to establish what U phases are present in the as-received residual waste; does the solubility of these phases control U release from residual waste, and how do the U phases evolve during leaching? To accomplish this goal, we used a combination of process knowledge, waste composition data, leach test data, and geochemical modeling to predict what phases are likely to control U release after tank closure.

Process knowledge indicates that process waste from the Bismuth Phosphate Plant were major components of the wastes disposed to tanks C-201, C-202, C-203, and C-204 [23]. The main U solids in tank sludge that resulted from this waste were $Na_4UO_2(CO_3)_3$ (čejkaite) and $NaUO_2PO_4{\cdot}xH_2O$ [24]. Micro-XRD analysis of water leached pre-retrieval waste indicated that the čejkaite had dissolved leaving a poorly crystalline Na uranate ($Na_2U_2O_7$) or clarkeite [$Na(UO_2)O(OH)H_2O_{0-1}$] phase [1,21,22].

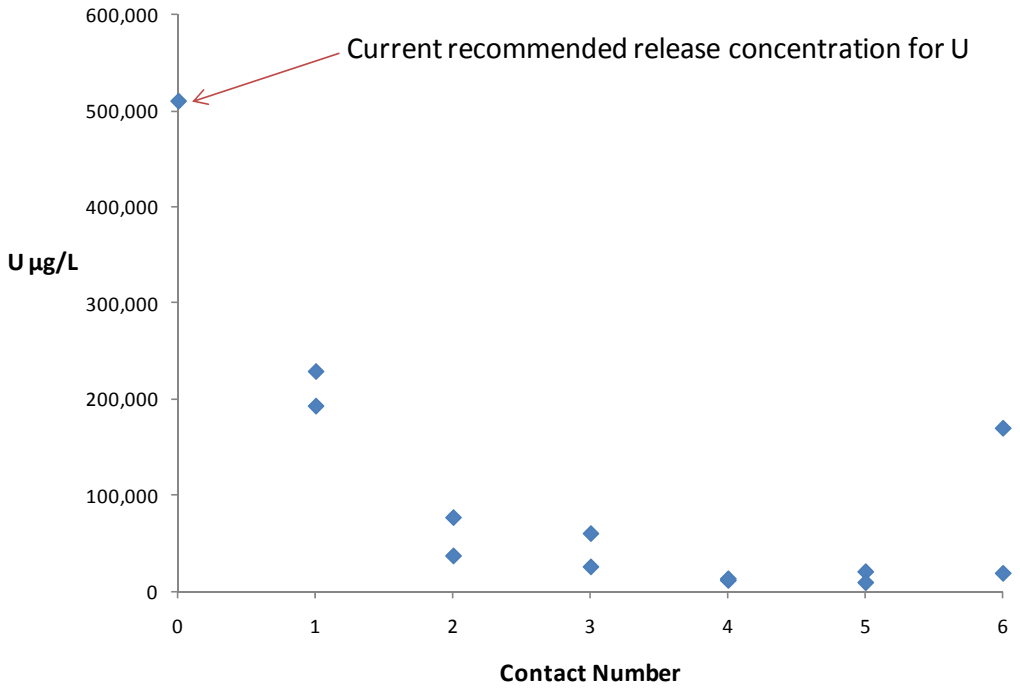

Fig. 4. Uranium concentrations measured in $CaCO_3$ leachants after contact with SST C-203 residual waste.

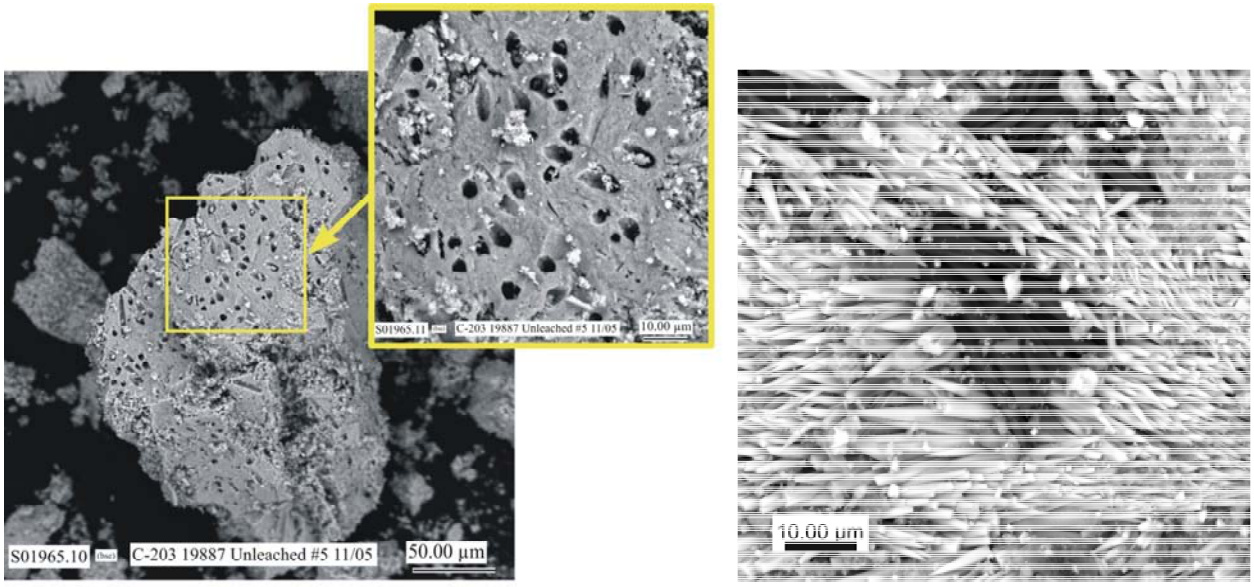

Fig. 5. Hexagonal čejkaite crystals that were found in SST C-203 pre-final retrieval waste (left) and hexagonal, rod-like dissolution cavities (right) that occur in a U rich particle found in the C-203 post-retrieval residual waste.

To illustrate how U phases in SSTs C-202 and C-203 sludge are likely to evolve during tank waste retrieval and subsequent leaching by infiltration after closure it is instructive to construct a thermodynamic stability field diagram. Fig. 6 is a thermodynamic stability field diagram created for U under conditions that are similar to some $CaCO_3$ leachates in contact with tank C-203 residual waste. In this case, the stability of U phases is shown as a function of sodium activity (a surrogate for concentration) and pH. Fixed parameters used to construct the diagram are log U = -3.0, log Ca = -8.0, log PO_4^{3-} = -6.0, log PCO_2 = -5.0, and log PO_2 = -3.6. For tank conditions prior to waste retrieval the supernatant contained very high sodium concentrations at very high pH values. Because the tanks were not sealed from the atmosphere, CO_2 was absorbed from the air into the supernatant, resulting in significant carbonate (CO_3^{2-}) concentrations entering the tank waste. Under these conditions Fig 6 indicates that čejkaite would be the most stable U phase. During the retrieval process for tanks C-202 and C-203, supernatant was pumped out and then a vacuum system was used to remove as much sludge as possible. After this step, a high-pressure water spray was used with a vacuum to remove as much additional sludge as possible. During this last stage of the process, the water contacting the sludge waste would have become relatively dilute, lowering the sodium concentration and pH. This would have caused the solution concentrations to move from the stability field of čejkaite into that of $Na_2U_2O_7$(am). This is consistent with the occurrence of poorly crystalline Na uranate ($Na_2U_2O_7$) or clarkeite [$Na(UO_2)O(OH)H_2O_{0-1}$] in the water leached pre-retrieval waste described earlier [1,22,23]. After final tank closure, it is conceivable that meteoric water could eventually contact the residual waste resulting in further dilution of pore fluids contacting the residual waste. The resulting decrease in sodium concentration and pH moves the chemistry into the stability field of schoepite ($UO_3 \cdot 2H_2O$) or similar phases such as meta-schoepite.

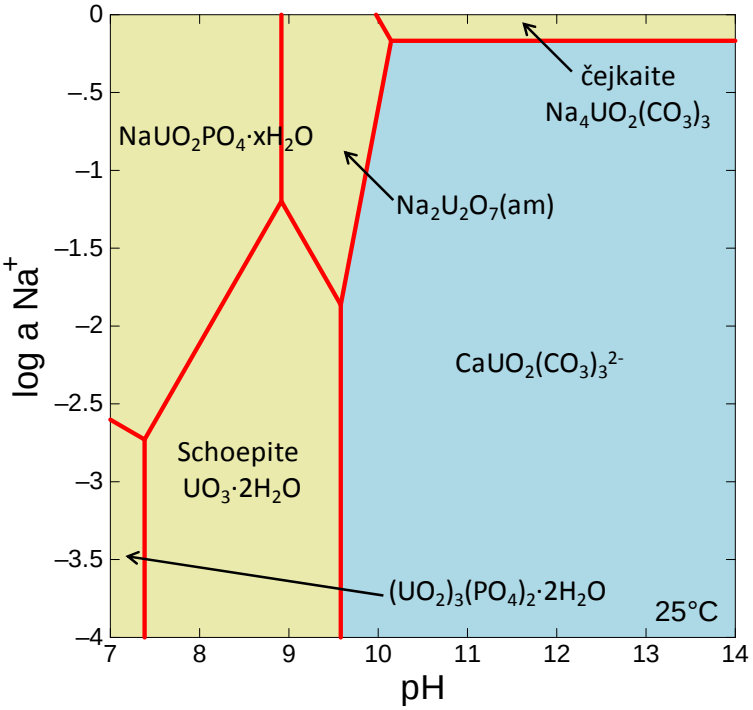

Fig. 6. Thermodynamic stability field diagram constructed to illustrate how U phases in SSTs C-202 and C-203 sludge are likely to evolve during retrieval and subsequent leaching by infiltration after closure (log U = -3.0, log Ca = -8.0, log PO_4^{3-} = -6.0, log PCO_2 = -5.0, and log PO_2 = -0.7).

This scenario is supported by solubility index calculations conducted on leachate solutions. Details of these calculations will be published in another research publication and are only summarized here. The SI calculation results indicate that as the DI and $CaCO_3$ leachant solutions contact residual waste any čejkaite remaining in the waste will dissolve and the solutions will come to equilibrium with $NaUO_2PO_4 \cdot xH_2O$ and $Na_2U_2O_7$(am). As further dilution occurs during subsequent leachant, the solutions remain in equilibrium with $NaUO_2PO_4 \cdot xH_2O$, but $Na_2U_2O_7$(am) dissolves and schoepite comes into equilibrium.

The situation for the $Ca(OH)_2$ leachates is very different. In this case, all U phases in the thermodynamic database were highly undersaturated with the exception of $CaUO_4$(c). The occurrence of this phase has not been verified, but the SI calculations indicate the solubility of this phase likely controls U release from our residual waste samples. It has been demonstrated that a number of U(VI)-Ca phases can form in alkaline solutions at room temperature, including becquerelite [$Ca(UO_2)_6O_4(OH)_6 \cdot 2H_2O$], $Ca_2UO_5 \cdot (H_2O)_{1.3\text{-}1.7}$, $CaUO_4$, Ca_3UO_6 , and CaU_2O_7 [25]. It was suggested the most likely phase at high pH in contact with $Ca(OH)_2$ solution is $Ca_2UO_5 \cdot (H_2O)_{1.3\text{-}1.7}$ [25]. It was later presumed this phase is a hydrated form of $CaUO_4$ with a variable water content ranging from $CaUO_4$ to $CaUO_4 \cdot (H_2O)_{0\text{-}1}$ [26]. More recent modeling of U(VI) precipitation experiments conducted in artificial cement pore waters and low-alkali pores waters indicated that amorphous Ca-uranate [$CaUO_4$(s)], with a solubility product of log $K_{SP}^0 = 23.1$, produced good agreement between the predicted solubility limits and experimental data for all solution compositions investigated [27].

Significantly lower solubility for $CaUO_4$(c) was observed in our leaching experiments. Using the critically reviewed value of log $K_{SP}^0 = 15.94$ for $CaUO_4$(c) provided in the database [4,28], reasonably good agreement between our experimental data and the modeling results was achieved. In addition to $CaUO_4$(s) precipitation, it is possible that some incorporation or co-precipitation of UO_2^{2+} into calcite or aragonite could have occurred in our $Ca(OH)_2$ leached experiments [29,30,31]. The residual wastes used in our experiments initially contain carbonate (as čejkaite and possibly Na_2CO_3). During contact with the $Ca(OH)_2$ leachant, calcium carbonate precipitation could have occurred. The solubility calculations indicate that calcite is oversaturated in stage 6 of the $Ca(OH)_2$ sequential leach tests. The impact of this process in our experiments is expected to be small because of the limited amount of carbonate in the waste and the weak partition coefficients for calcite exhibited by U (0.01 to 0.26) [32].

Fig. 7 is a thermodynamic stability field diagram constructed to illustrate U phases in SSTs C-202 and C-203 residual waste that are likely to control U release during leaching with $Ca(OH)_2$ as a function of Ca activity and pH. Fixed parameters used to construct the diagram are log U = -4.0, log Na = -1.5, log PO_4^{3-} = -4.0, log PCO_2 = -7.5, and log PO_2 = -3.6. For these conditions, the diagram indicates that $CaUO_4 \cdot (H_2O)_{0\text{-}1}$ is stable at relatively high pH values relative to autunite and $NaUO_2PO_4 \cdot xH_2O$. In addition, autunite is more stable than $NaUO_2PO_4 \cdot xH_2O$ at high Ca concentrations.

CONCLUSIONS

Investigations of contaminant release from Hanford tank residual waste have indicated that in some cases certain contaminants of interest (Tc and Cr) exhibit inhibited release. The percentage of Tc that dissolved from residual waste from SSTs C-103, C-106, C-202, and C-203 ranged from approximately 6 % to 10 %. The percent leachable Cr from residual waste from tanks C-103, C-202, and C-203 ranged from approximately 1.1 % to 44 %. Solid phase characterization results indicate that the recalcitrant forms of these contaminants are associated with Fe oxides. XANES analysis of Tc and Cr in residual waste indicates that these contaminants occur in Fe oxide particles as their lower, less-soluble oxidation

states [Tc(IV) and Cr(III)]. The form of these contaminants is likely as oxides or hydroxides incorporated within the structure of the Fe oxide.

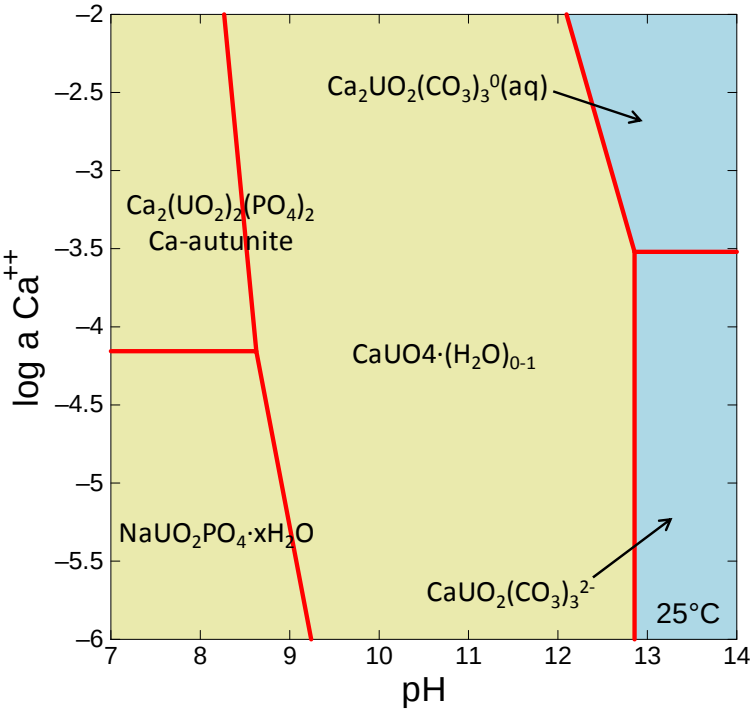

Fig. 7. Thermodynamic stability field diagram constructed to illustrate U phases in SST C-202 and C-203 residual waste that are likely to control U release during leaching with $Ca(OH)_2$ (log U = -4.0, log Na = -1.5, log PO_4^{3-} = -4.0, log PCO_2 = -7.5, and log PO_2 = -0.7).

Leaching behavior of U from tank residual waste was studied using DI water, and $CaCO_3$ and $Ca(OH)_2$ saturated solutions as leachants. The release behavior of U from tank residual waste is complex. Initial U concentrations in water and $CaCO_3$ leachants are high due to residual amounts of the highly soluble U mineral čejkaite. As leaching and dilution occur $NaUO_2PO_4 \cdot xH_2O$, $Na_2U_2O_7$(am) and schoepite (or a similar phase) become the solubility controlling phases for U.

In the case of the $Ca(OH)_2$ leachant, U release from tank residual waste is dramatically reduced. Thermodynamic modeling indicates the solubility of $CaUO_4$(c) likely controls release of U from residual waste in the $Ca(OH)_2$ leachants. It is assumed the solubility controlling phase is actually a hydrated version of $CaUO_4$ with a variable water content ranging from $CaUO_4$ to $CaUO_4 \cdot (H_2O)$. The critically reviewed value for $CaUO_4$(c) (log K_{SP}^0 = 15.94) [4,28] produced good agreement with our experimental data for the $Ca(OH)_2$ leachates.

ACKNOWLEDGMENTS

The authors acknowledge M. Connelly at Washington River Protection *Solutions* LLC (Richland, Washington) for providing project funding and technical guidance. Pacific Northwest National Laboratory is operated for DOE by Battelle Memorial Institute under contract DE-AC05-76RL01830. Synchrotron-based analyses were completed at the XSD/PNC beamline 20-ID at the Advanced Photon Source; the PNC CAT project is supported by funding from DOE's Office of Basic Energy Sciences, the

University of Washington, Simon Fraser University, and the Natural Sciences and Engineering Research Council of Canada. Use of the Advanced Photon Source is supported by DOE's Office of Science, Office of Basic Energy Sciences, under contract DE-AC02-06CH11357.

REFERENCES

1. W. J. DEUTSCH, K. M. KRUPKA, M. J. LINDBERG *et al.*, *Hanford Tanks 241-C-203 and 241-C-204: Residual Waste Contaminant Release Model and Supporting Data,* PNNL-14903, Pacific Northwest National Laboratory, Richland, Washington (2004).
2. K. J. CANTRELL, K. M. KRUPKA, W. J. DEUTSCH *et al.*, *Hanford Tank 241-C-103 Residual Waste Contaminant Release Models and Supporting Data,* PNNL-16738, Pacific Northwest National Laboratory, Richland, Washington (2008).
3. W. J. DEUTSCH, K. M. KRUPKA, M. J. LINDBERG *et al.*, *Hanford Tanks 241-C-202 and 241-C-203 Residual Waste Contaminant Release Models and Supporting Data,* PNNL-16229, Pacific Northwest National Laboratory, Richland, Washington (2007).
4. C. BETHKE and S. YEAKEL, *The Geochemist's Workbench, Release 8.0, Reference Manual*, Hydrogeology Program, Urbana, Illinois (2009).
5. A. R. FELMY, Y. XIA, Z. WANG, "The solubility product of $NaUO_2PO_4 \cdot xH_2O$ determined in phosphate and carbonate solutions," *Radiochimica Acta,* vol. 93, no. 7, pp. 401-408 (2005).
6. D. RAI, A. R. FELMY, N. J. HESS, V. L. LEGORE, D. E. MCCREADY, "Thermodynamics of the U(VI)-Ca^{2+}-Cl^--OH^--H_2O system: Solubility product of becquerelite," *Radiochimica Acta,* vol. 90, pp. 495-503 (2002).
7. T. YAMAMURA, A. KITAMURA, A. FUKUI, S. NISHIKAWA, T. YAMAMOTO, H. Moriyama, "Solubility of U(VI) in highly basic solutions," *Radiochimica Acta,* vol. 83, pp. 139-146 (1998).
8. F. CHEN, R. C. EWING, S. B. CLARK, "The Gibbs free energies and enthalpies of formation of U^{6+} phases: An empirical method of prediction," *American Mineralogist*, vol. 84, no. 4, pp. 650-664 (1999).
9. D. GORMAN-LEWIS, P. C. BURNS, J. B. FEIN, "Review of uranyl mineral solubility measurements," *J. Chem. Thermodynamics*, vol. 40, pp. 335-352 (2008).
10. A. K. ALWAN, P. A. WILLIAMS, "The aqueous chemistry of uranium minerals. Part 2. Minerals of the liebigite group," *Mineralogical Magazine*, vol. 43, pp. 665-667 (1980).
11. D. GORMAN-LEWIS, T. SHVAREVA, K. A. KUBATKO, *et al.,* "Thermodynamic properties of autunite, uranyl hydrogen phosphate, and uranyl orthophosphate from solubility and calorimetric measurements," *Environ. Sci. Technol.*, vol. 43, pp. 7416-7422, (2009).
12. W. DONG, S. C. BROOKS, "Determination of the formation constants of ternary complexes of uranyl and carbonate with alkaline earth metals (Mg^{2+}, Ca^{2+}, Sr^{2+}, and Ba^{2+}) using anion exchange method," *Environ. Sci. Technol*., vol. 40, pp. 4689-4695 (2006).
13. W. J. DEUTSCH, K. M. KRUPKA, M. J. LINDBERG *et al.*, *Hanford Tank 241-C-106: Residual Waste Contaminant Release Model and Supporting Data,* PNNL-15187, Rev. 1, Pacific Northwest National Laboratory, Richland, Washington (2007).
14. W. J. DEUTSCH, K. M. KRUPKA, M. J. LINDBERG *et al.*, *Hanford Tank 241-C-106: Impact of Cement Reactions on Release of Contaminants from Residual Waste,* PNNL-15544, Pacific Northwest National Laboratory, Richland, Washington (2006).
15. W. J. DEUTSCH, K. J. CANTRELL, and K. M. KRUPKA, *Contaminant Release Data Package for Residual Waste in Single-Shell Hanford Tanks,* PNNL-16748, Pacific Northwest National Laboratory, Richland, Washington (2007).
16. K. J. CANTRELL, K. M. KRUPKA, K. N. GEISZLER *et al.*, *Hanford Tank 241-S-112 Residual Waste Composition and Leach Test Data,* PNNL-15793, Pacific Northwest National Laboratory, Richland, Washington (2008).

17. K. J. CANTRELL, K. M. KRUPKA, W. J. DEUTSCH *et al.*, "Residual waste from Hanford tanks 241-C-203 and 241-C-204. 2. Contaminant release model," *Environ. Sci. Technol.,* vol. 40, no. 12, pp. 3755-3761 (2006).
18. B. WAKOFF, K. L. NAGY, "Perrhenate uptake by iron and aluminum oxyhydroxides: An analogue for pertechnetate incorporation in Hanford waste tank sludges," *Environ. Sci. Technol.,* vol. 38, no. 6, pp. 1765-1771 (2004).
19. P. C. ZHANG, K. L. KRUMHANSL, P. V. BRADY, "Boehmite sorbs perrhenate and pertechnetate," *Radiochimica Acta*, vol. 88, pp. 369-373 (2000).
20. F. N. SKOMURSKI, K. M. ROSSO, K. M. KRUPKA, B. P. MCGRAIL, "Technetium incorporation into hematite (α-Fe_2O_3)," *Environ. Sci. Technol.,* 2010, vol. 44, no. 15, pp 5855-5861 (2010).
21. W. J. DEUTSCH, K. M. KRUPKA, K. J. CANTRELL *et al.*, *Advances in Geochemical Testing of Key Contaminants in Residual Hanford Tank Waste,* PNNL-15372, Pacific Northwest National Laboratory, Richland, Washington (2005).
22. K. M. KRUPKA, H. T. SCHAEF, B. W. AREY *et al.*, "Residual waste from Hanford tanks 241-C-203 and 241-C-204. 1. Solids characterization," *Environ. Sci. Technol.,* vol. 40, no. 12, pp. 3749-3754 (2006).
23. M. E. JOHNSON, *Origin of Wastes in C-200 Series Single-Shell Tanks,* RPP-15408, CH2M HILL Hanford Group, Richland, Washington (2003).
24. U.S. ATOMIC ENERGY COMMISION. *Uranium Recovery Technical Manual*, Declassified Document, HW-19140, General Electric Company, Richland, Washington (1951).
25. M. ATKINS, A. N. BECKLEY, F. P. GLASSER, "Influence of cement on the near field environment and its specific interactions with uranium and iodine," *Radiochimica Acta,* vol. 44/45, pp. 255-261 (1988).
26. L. P. MORONI, F. P. GLASSER, "Reactions between cement components and U(VI) oxide," *Waste Management,* vol. 15, no. 3, pp. 243-254 (1995).
27. J. TITS, T. FUJITA, M. TSUKAMOTO, E. WIELAND, "Uranium(VI) uptake by synthetic calcium silicate hydrates," *Mater. Res. Soc. Symp. Proc.,* vol. 1107, pp. 467-474, (2008).
28. I. GRENTHE, J. FUGER, R. J. M. KONINGS *et al., Chemical Thermodynamics, Volume 1: Chemical Thermodynamics of Uranium,* North-Holland, Amsterdam, (1992).
29. R. J. REEDER, M. NUGENT, G. M. LAMBLE et al., "Uranyl-incorporation into calcite and aragonite: XAFS and luminescence characterization," *Environ. Sci. Technol.*, vol. 34, no. 4, pp. 638-644 (2000).
30. R. J. REEDER, M. NUGENT, C. D. TAIT et al., "Coprecipitation of uranium(VI) with calcite: XAFS, micro-XAS, and luminescence characterization," *Geochim. Cosmochim. Acta*, vol. 65, no. 20, pp. 3491-3503 (2001).
31. D. E. MEECE, L. K. BENNINGER, "The coprecipitation of Pu and other radionuclides with $CaCO_3$," *Geochim. Cosmochim. Acta*, vol. 57, no. 7, pp. 1447-1458 (1993).
32. E. CURTI, "The coprecipitation of radionuclides with calcite: estimation of partition coefficients based on review of laboratory investigations and geochemical data," *Appl. Geochem.*, vol. 14, no. 4, pp. 433-445 (1999).